

## ATOMIC FORCE MICROSCOPY:

### GENERAL PRINCIPLES AND A NEW IMPLEMENTATION

Gary M. McClelland, Ragnar Erlandsson, and Shirley Chiang

IBM Almaden Research Center  
650 Harry Road  
San Jose, CA 95120

### INTRODUCTION

Recently, Binnig, Quate, and Gerber developed the atomic force microscope (AFM), an instrument which senses minute ( $10^{-12}$  -  $10^{-8}$  N) forces between a sharp tip and a sample surface [1]. In addition to enabling the study of solid-solid interactions on a unprecedentedly small scale, the AFM provides a general method for doing non-destructive surface profilometry at a resolution better than 10 nm and perhaps down to the atomic level. In this paper we review the principles of the AFM, discuss its potential resolution and data rate, describe our new AFM design, and present some initial results. We have obtained three dimensional surface profiles with 20 nm lateral resolution, which to our knowledge is better than what has been attained previously by stylus profilometry.

The AFM was developed as a variant of the scanning tunneling microscope (STM) [2]. The STM, developed by Binnig, Rohrer, Gerber and Weibel [3], is the first instrument capable of directly obtaining three dimensional (3D) images of solid surfaces with atomic resolution. In the STM, a tunneling current is sensed between a conducting solid and a sharp metal tip held 0.3 - 1 nm above the solid surface. Because the current increases by approximately a factor of 10 for each 0.1 nm, the tip is brought closer to the surface; the tunneling current is a very sensitive measure of the tip-surface distance. To image a sample surface, two piezoelectric drivers raster the tip parallel to the xy plane of the sample. A feedback loop drives a third piezoelectric element along the z direction perpendicular to the sample to adjust the tip position to keep the current, or roughly speaking, the tip-surface separation, constant. The tip position  $z(x,y)$  gives a three dimensional image of the sample surface. With proper interpretation of the tunneling current as a function of the tip separation and voltage, electronic properties of the surface such as the work function and the energy of the surface electronic states can also be deduced [2].

The ability of the STM to obtain 0.2 nm resolution parallel and 0.01 nm perpendicular to the surface can be attributed to four features: 1. Piezoelectric transducers can achieve resolution better than 0.01 nm over a range of several microns. 2. The mechanical drift rates attainable (less than 1 nm/minute) are insignificant or can be corrected for over the typical image acquisition time of 1 s to 5 minutes. 3. Vibration isolation prevents building vibration and acoustic noise from affecting the sample-tip assembly. 4. The rapid variation of the tunneling current with distance localizes the current at the very end of the tip.

In designing the atomic force microscope [1], Binnig *et al.* created another high resolution profiling device by using the first three features of the STM listed above and detecting the force between the sample and tip rather than the tunneling current to sense the proximity of the tip to the sample (Fig. 1). In their AFM, a diamond tip is mounted on a small electrically conducting cantilever, which bends due to the force exerted by the sample on the tip. The lever's deflection is sensed by the the current from the lever to a nearby tunneling tip. To characterize the spatial dependence of the tip-sample force, the sample is scanned across the tip, while the tip-sample distance is adjusted to keep the deflection of the cantilever constant. Alternatively, the sample can be vibrated slightly along  $z$  and, by following the amplitude of the induced lever oscillation, a 3D surface of constant force derivative  $F'$  determined. Since exceedingly small deflections of the cantilever can be detected, very small forces can be measured. Operating at a force of  $10^{-8}$  N, Binnig *et al.* attained a resolution of  $\approx 10$  nm parallel and  $\approx 0.1$  nm perpendicular to the surface. Using a related technique, Dürig *et al.* have characterized the force between the tip and the sample in a STM by fabricating the sample into a cantilever [4].

Because the contours of the tip-sample force closely follow the surface topography, the AFM can be used as a very high resolution 3D profilometer, and as such it can be compared to several other techniques. In this application, the AFM is similar to a conventional stylus profilometer [5], which however has much poorer spatial resolution and works only with repulsive forces several orders of magnitude larger than can be detected by the AFM. The STM has so far achieved better spatial resolution than the AFM, but it can only be used with electrical conductors. The scanning electron microscope can readily operate at a wide range of magnifications but must be used in a vacuum and can obtain 3D information only indirectly, by shadowing. A conventional scanning optical microscope can obtain direct, non-contact 3D images, but its resolution is limited to a substantial fraction of the wavelength of light [6]. However, the near-field optical scanning microscope has attained a resolution as small as 20 nm [7]. Working at room temperature, acoustic microscopes have a lateral resolution on the order of  $0.5 \mu\text{m}$ , but by using liquid helium as a operating medium the resolution can be enhanced to better than 20 nm [8].

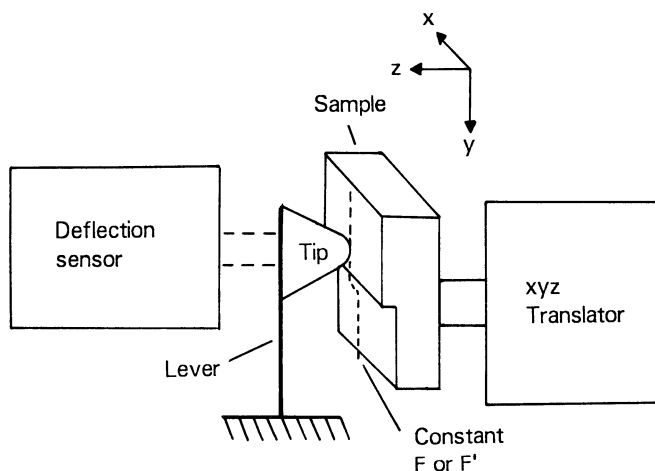


Fig. 1. Schematic diagram of the atomic force microscope. Forces between the tip and sample cause the deflection of the lever, which can be measured by tunneling as in reference [1], or by optical interference, as described here.

The AFM goes beyond the capabilities of simple profilometry, because it can quantitatively measure physical, chemical, magnetic, frictional, and electrostatic interfacial forces with very high spatial resolution. In this application, the AFM is related to a device introduced nearly 20 years ago by Tabor and Winterton [9] and developed by Israelachvili and coworkers [10]. Their technique works with significantly larger forces ( $> 10^{-6}$  N) and foregoes lateral resolution by using a well-defined interfacial geometry of two crossed mica cylinders 1 cm in radius.

## THEORY

Compared to other forces which are commonly measured directly, interatomic forces are not as small as might be expected. The force required to break a typical chemical bond is on the order of  $400 \text{ kJoule mole}^{-1}/0.1 \text{ nm} \approx 10^{-8} \text{ N}$ . (note:  $1 \text{ N} = 10^5 \text{ dyne} \approx 10^2 \text{ gm.}$ ). The associated force constant is about  $100 \text{ N/m}$  or  $100 \text{ gm/cm}$ , of the same order of magnitude as a conventional spring. The force exerted between two solid bodies can be considerable even if no chemical or metallic bonds are formed between them [11]. When such surfaces are closer than about  $0.3 \text{ nm}$ , the force is repulsive. At longer distances the attractive dispersion interaction causes a force which arises from the interaction between the electric dipole zero point fluctuations of one solid with the electric polarization induced in the other solid. Between about  $0.3$  and  $10 \text{ nm}$ , the attractive interaction potential can be reasonably approximated by integrating the dispersion potential over the volumes of the two solids:

$$V = - \int \frac{A}{(\vec{r}_1 - \vec{r}_2)^6} d^3\vec{r}_1 d^3\vec{r}_2. \quad (1)$$

Here  $A$  is the Hamaker constant, which for different material combinations varies from  $0.4$  to  $4 \times 10^{-19} \text{ joules}$  [11]. Because of retardation effects due to the finite speed of light, the interaction potential drops off faster than this equation indicates at distances larger than  $10 \text{ nm}$ .

There is a great advantage to operating the AFM in such a way as to sense the long range attractive rather than the short range repulsive tip-sample potential, because the weak attractive potential is much less likely to cause damage to the tip or sample. To simulate the operation of the AFM while sensing this attractive potential, consider a flat sample interacting with a conical tip terminating in a spherical end of radius  $R$  (Fig. 1). Because the interaction potential falls off so rapidly with increasing distance, if the distance  $z$  between the tip and the solid is less than  $R$ , the potential between the tip and the solid can be approximated by applying Eq. (1) to a sphere and a half space, which gives

$$V = - \frac{AR}{6z}. \quad (2)$$

Using  $A = 5 \times 10^{-20} \text{ J}$ ,  $R = 1.5 \text{ nm}$ , and  $z = 0.5 \text{ nm}$ , the attractive potential, the force, and the force derivative are  $2.5 \times 10^{-20} \text{ joules}$ ,  $5 \times 10^{-11} \text{ N}$ , and  $0.2 \text{ N/m}$ , respectively.

Assuming that forces of this magnitude could be detected with the AFM, the most useful measure of the performance of the AFM as a profiling device is the lateral resolution parallel to the surface attained by following the 3D locus of constant force derivative  $F'$  as the tip is scanned along the surface (Fig. 1). A useful measure of this resolution is the width of the step this locus makes as it follows an abrupt monatomic step in the surface. For the tip just described, starting on the contour  $0.5 \text{ nm}$  above the flat surface, the half-width (the spacing between 25 and 75 % rise) of such a step is  $0.6$

nm [12]. Thus the tip-sample potential contains very high resolution information about the geometry of the surface.

Whether the sharp features of the tip-surface potential can be measured depends on the signal-to-noise ratio of the AFM. The most important parameter affecting this ratio is the force constant  $k_\ell$  of the lever. Although it would appear best to use the weakest lever possible in order to attain the maximum deflection, two criteria in fact place a lower bound on the usable lever stiffness: 1. If the downward curvature of the attractive tip-sample potential is ever greater than the upward curvature  $k_\ell$  of the lever's harmonic potential, the dependence of the tip-sample separation on the sample position will not be continuous or reversible, and the lever will suddenly jump into contact with a slowly approaching sample [9,10]. 2. The thermally excited excitation of the lever, whose amplitude is given by the equipartition theorem as

$$A_T = \sqrt{\frac{2k_B T}{k_\ell}}, \quad (3)$$

must be kept small compared to  $z$ . Here  $k_B$  is Boltzmann's constant and  $T$  is the temperature. According to this expression, maintaining a mean thermal amplitude of 0.03 nm at 300 K requires  $k_\ell = 10$  N/m, a surprisingly large value. For sharp tips, this force constant is also large enough to satisfy the first criteria above.

Even if the deflection of the lever can be measured exactly, there remains a source of noise due to fluctuations in the thermally excited vibration, and we now present a heuristic estimate of this noise. Modelling the lever as a simple damped harmonic oscillator, with resonant frequency  $\omega_\ell$  and quality factor  $Q$ , the strength of the coupling to the heat bath is inversely proportional to  $Q$ , which also determines the time  $\tau_D = Q/\omega_\ell$  for the decay of any excitation at  $\omega_\ell$  in the lever. Thus we can think of the thermal noise as independently exciting the lever with random phase at intervals  $\tau_D$ . Averaging noise at frequency  $\omega_\ell$  over a time  $t$  is like making  $\frac{t}{\tau_D}$  independent measurements of a variable with root mean square thermal amplitude  $A_T$  and average 0. The root mean square average of such a series of measurements is the noise

$$N = A_T / \sqrt{t/\tau_D} = \sqrt{\frac{2k_B T}{k_\ell}} \sqrt{\frac{t\omega_\ell}{Q}}. \quad (4)$$

Suppose that the AFM is operated by vibrating the sample at  $\omega_\ell$  with amplitude  $A_S$ . This modulation technique not only enhances the lever deflection; it essentially eliminates the effect of low frequency mechanical drift on the force measurement. Including the resonant enhancement, the induced motion in the lever is the signal  $S = A_S F' Q / k_\ell$ , where  $F'$  is the normal derivative of the tip-sample force. Using the expressions above, the signal to noise ratio for an averaging time  $t$  is

$$S/N = \sqrt{\left(\frac{1}{2k_B T}\right) \left(\frac{F'^2 A_S^2}{k_\ell}\right) (\omega_\ell Q) t}. \quad (5)$$

The exact result [12] is a factor of  $1/\sqrt{2}$  smaller than this expression. Because the thermal noise has a white spectrum, the thermally determined  $S/N$  limit is independent of the modulation frequency, as long as the lever behaves as a simple harmonic oscillator [12]. However, it will often be advantageous to vibrate the sample at the lever resonant frequency, since the resulting enhanced lever motion will then be easier to detect.

Eq. (5) has been factored to clarify the role of each experimental variable in determining the performance of the AFM. The first term can be in-

creased only by cooling the instrument. The sample-tip interaction determines  $F'$ , and the need to keep both the intentionally induced and thermal relative vibration of the tip and sample small puts an upper bound on  $A_s$  and a lower bound on  $k_f$ .

Given that the lever force constant cannot be decreased indefinitely, the major opportunity for increasing S/N is through increasing the resonant frequency  $\omega_f$  and quality factor  $Q$  of the lever. As an example, we compare the performance of two levers in obtaining a surface image, using a small sample oscillation  $A_s = 0.05$  nm and these parameters derived above:  $k_f = 10$  N/m and  $F' = 0.2$  N/m. The value of  $Q$  depends strongly on how the lever is supported; we use a value of 200 in all that follows. First consider a tungsten lever  $0.12 \times .002 \times .002$  cm, which is easily manufactured by standard machine tools and has a resonant frequency of 11 kHz. Using this lever at 300 K with a 10 ms averaging time, Eq. (5), corrected by  $1/\sqrt{2}$ , predicts  $S/N = 10$ , corresponding to a vertical uncertainty of 0.02 nm. Generating a three dimensional surface  $z(x,y)$  of constant  $F'$  over a matrix of  $300 \times 300$  (x,y) positions would require 1000 s at 300 K and 13 s at 4 K.

Smaller levers with their higher resonant frequencies have much lower noise levels, which lead to faster data acquisition times. Consider a silicon lever with dimensions  $2 \times 2 \times 0.1$   $\mu\text{m}$ , which could be manufactured by techniques used for integrated circuits [13]. This lever has the same force constant as the larger tungsten lever but a resonant frequency of 37 MHz. Using the silicon lever, a  $300 \times 300$  image can be recorded in 300 ms at 300 K and 4 ms at 4 K. Mechanical drift is essentially negligible over these time scales. Remember that these rates apply to a tip sensing the weak dispersion forces from the sample. If the tip was allowed to "touch" the sample and interact with the hard repulsive edge of the potential, the resulting larger forces would give much higher data rates, perhaps at the risk of damaging the tip and sample.

## APPARATUS

Although the tunneling method employed by Binnig *et al.* [1] is clearly an extremely sensitive means for detecting the lever deflection, any method which contributes a noise level below the fundamental thermal noise gives potentially the same AFM performance. In our apparatus, (Fig. 2), we use optical interference to sense the lever position. This is a more reliable and easily implemented detection method than tunneling. Because the optical method senses a large (1  $\mu\text{m}$ ) region of the lever, it is much less sensitive to the roughness of the lever. Thus the optical technique is less affected by thermal drift than is tunneling, which is sensitive to movements of a rough lever parallel as well as perpendicular to the surface. Unlike tunneling, the optical technique does not require an electrically conductive lever. However, the tunneling method for lever detection does have the potential advantage that it can be used with levers smaller than the wavelength of light.

In our design, a helium neon laser beam is sent through a 4 % reflecting flat and focussed by a microscope objective on the lever. Light reflected from the lever and recollimated by the lens combines with the beam reflected off the flat to form an interference pattern, which is detected by the photodiode. For two beams of equal intensity  $90^\circ$  out of phase, a change in position of the lever of 0.01 nm alters the light intensity by .02 %, an amount which can be easily detected if it is modulated at frequencies  $> 100$  Hz.

Following the STM design used in our laboratory [14], the sample is mounted on three orthogonal piezoelectric tubes, two of which (x and y) raster the sample in the surface plane while the third (z) moves the sample toward

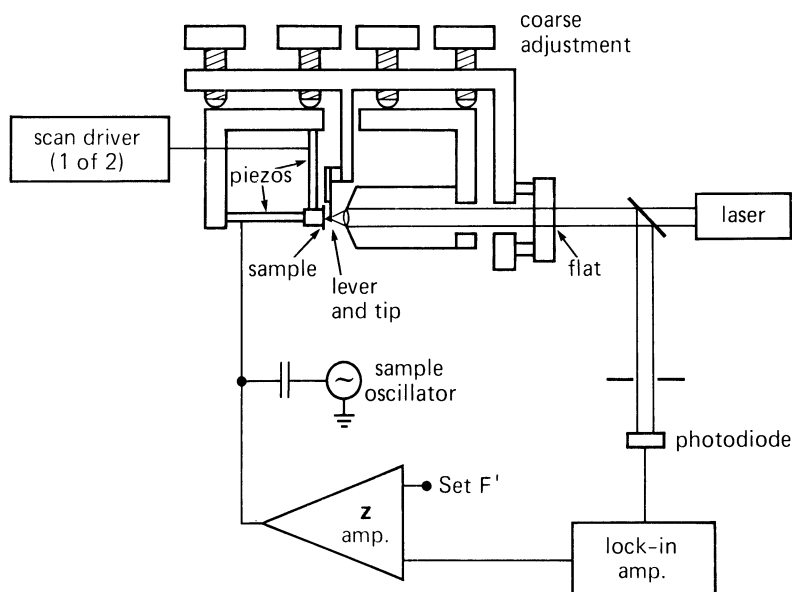


Fig. 2. Our AFM design, which uses optical interference to detect the lever deflection. A feedback loop keeps the perpendicular force derivative between the sample and the tip constant. Excluding the external optics and electronics, the AFM is about 12 cm long.

and away from the tip. The data presented here were obtained by applying a small AC voltage to the z tube to induce an oscillation in the sample and, through the force coupling, to the lever. The resultant oscillation in the photodiode signal is converted by the lockin amplifier to a voltage which is proportional to  $F'$ . The z amplifier compares the voltage to some preset value and drives the z tube to form a feedback loop to maintain  $F'$  constant.

Adopting the principle of a conventional kinematic mirror mount, both the sample with its three drive tubes and the objective are mounted in holders which are supported and coarsely translated by three fine adjusting screws which can move the sample and lens in increments less than  $2\ \mu\text{m}$ . This allows the sample to be moved within the  $2.5\ \mu\text{m}$  operating range of the z piezoelectric tube without crashing the sample into the tip. For adjustment of the phase of the interference signal, the flat is also mounted on a piezoelectric translator. To enable other types of modulation techniques [1,10] the lever can be vibrated directly by its own piezoelectric mount. Our AFM was isolated from building vibrations by mounting it on a stack of five 6 mm thick steel plates separated by sets of four small viton rubber spacers [15]. Since the stainless steel framework is quite heavy, the natural vibrational frequencies of this mounting system were below 10 Hz, indicating effective isolation from higher frequencies which could excite the lever. The AFM and plate assembly were mounted on a conventional pneumatically isolated optical table and enclosed for sound insulation by a plastic box. With the box removed we can observe the approach of the tip to a selected position on the sample with the aid of a conventional optical microscope. To enable the use of well-characterized samples and improve thermal and acoustic isolation, the AFM will eventually be enclosed in an ultrahigh vacuum chamber.

## RESULTS

Our first experiments were designed to characterize the general operation of our instrument rather than to realize the ultimate capabilities of the AFM calculated above. The first sample was cleaved pyrolytic graphite, and the lever was formed from a 3 mm long, 75  $\mu\text{m}$  diameter tungsten wire with its end bent at 90° and electrolytically etched [16] to form a tip. We studied the graphite - tungsten system because it has been the subject of many high resolution STM investigations [17,18], including some which have obtained atomic resolution in air [18]. There is good evidence that large forces between the tip and sample [19] may play a role in forming the STM image for the tungsten-graphite [20] and tungsten-silver [4] systems.

To obtain the AFM images of Fig. 3, we aligned the tip with a poorly cleaved rough area of the sample in order to insure some structure larger than the atomic level. Figure 3 shows two 3D images of the sample surface. The sample was modulated at a frequency different than that of the lever resonance to induce a lever oscillation of amplitude 0.1 nm, which corresponds to a force modulation of about  $3 \times 10^{-9}\text{N}$ . Once our electronics and laser are optimized, we expect to be able to work with forces a factor of 100 smaller. Figure 3a was obtained with a tip dulled by repeated hard contact with the sample. The surface includes a broad valley 100 nm deep, which contains several features as small as 150 nm in width running parallel to the valley. Figure 3b shows another region of the same sample profiled with a freshly etched and presumably sharper tip. Here, some features (e.g. at the top, just left of center) show a resolution parallel to the surface as small as 20 nm, while the noise level perpendicular to the surface is 1 nm. Although each of these frames were acquired over a period of several minutes, the signal to noise of our interference signal was good enough to acquire these plots in a few seconds.

Although we believe the data of Fig. 3b represents the highest lateral resolution three dimensional surface profile ever recorded by direct force sensing, it does not offer a conclusive test of the resolving capabilities of the AFM. For this we require a sample with well characterized surface features. To spatially calibrate our instrument, we hope to measure the surface topography of a sample by applying a voltage between the tip and the sample and operating the instrument as a STM to obtain a tunneling image.

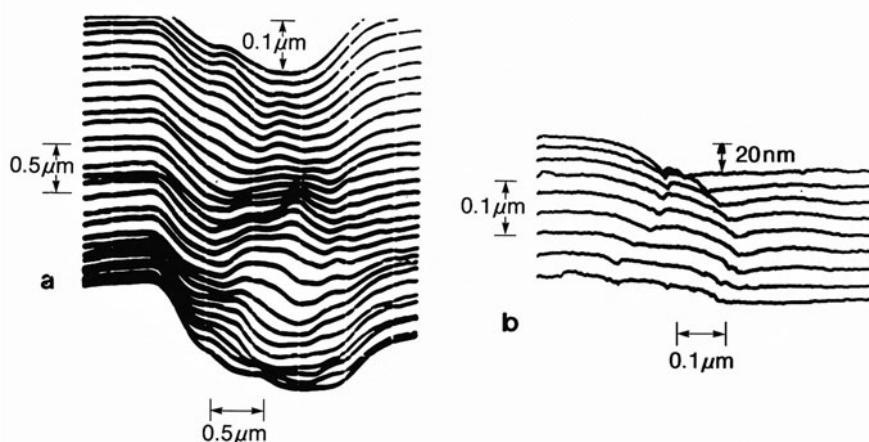


Fig. 3. Two images of a graphite surface. Each curve is a plot of the z coordinate of the tip as a function of the x coordinate in the surface plane, holding y constant. Successive curves are obtained by regularly incrementing y.

This could be compared to a force image obtained immediately afterward on the same sample area. In addition, we plan to calibrate the force sensitivity of the instrument by using electric or magnetic forces.

The ultimate achievement of the AFM would be to resolve individual atoms. The atomic resolution of the STM while using tips with a nominal radius of  $> 25$  nm has generally been attributed to the very strong distance dependence of the tunneling current. Tunneling occurs through only a single atom or small group of atoms which is closest to the sample. The attractive dispersion force, with its  $1/r^7$  distance dependence, is not so rapidly varying that a very small region of the tip will dominate the force signal, as it does the tunneling current. However, at the risk of damaging the tip or sample, the AFM can also operate with the short range repulsive forces. Because this force increases quite dramatically with distance, we believe that by mapping the repulsive force the AFM should be able to attain atomic resolution.

#### ACKNOWLEDGEMENTS

We thank D. J. Auerbach, G. Binnig, G. Castro, Ch. Gerber, E. C. Teague, M. A. Trump, and R. J. Wilson for helpful discussions and B. A. Hoenig for technical assistance.

#### REFERENCES

1. G. Binnig, C. F. Quate and Ch. Gerber, Phys. Rev. Lett. 12, 930 (1986).
2. G. Binnig and H. Rohrer, IBM J. Res. and Develop. 30, 355 (1986); C. F. Quate, Physics Today 39, 26 (1986).
3. G. Binnig, H. Rohrer, Ch. Gerber and E. Weibel, Phys. Rev. Lett. 49, 57 (1982).
4. U. Dürig, J. K. Gimzewski, and D. W. Pohl, Phys. Rev. Letts., to be published.
5. E. C. Teague, F. E. Scire, S. M. Baker, and S.W. Jensen, Wear 83, 1 (1982). J. M. Bennet and J. H. Dancy, Appl. Opt. 20, 1785 (1981).
6. G. S. Kino, P. C. D. Hobbs, and T. Corle, this volume; J. C. Wyant, C. L. Koliopoulos, B. Bhusan, and O. E. George, ASLE Trans. 27, 101 (1984).
7. U. Dürig, D. W. Pohl, and F. Rohner, J. Appl. Phys. 59, 3318 (1986).
8. C. F. Quate, Phys. Today 38, 34 (1985).
9. D. Tabor and R. H. S. Winterton, Proc. R. Soc. London A 312, 435 (1969).
10. See, for example, R. G. Horn and J. N. Israelachvili, J. Chem. Phys. 75, 1400 (1981).
11. A. W. Adamson, "Physical Chemistry of Surfaces," Wiley, New York (1976); J. N. Israelachvili, "Intermolecular and Surface Forces," Academic Press, London (1985).
12. G. M. McClelland, to be published.
13. K. E. Peterson, Proc. IEEE, 70, 420 (1982).
14. S. Chiang and R. J. Wilson, IBM J. Res. and Develop. 30, Sept. (1986).
15. Ch. Gerber, G. Binnig, H. Fuchs, O. Marti, and H. Rohrer, Rev. Sci. Instrum. 57, 221 (1986).
16. R. Gomer, "Field Emission and Field Ionization," Harvard University Press, Cambridge (1961); E. W. Müller and T. T. Tsong, "Field Ion Microscopy, Principles and Applications," Elsevier, New York (1969).
17. G. Binnig, H. Fuchs, Ch. Gerber, H. Rohrer, E. Stoll, and E. Tosatti, Europhys. Lett. 1, 31 (1986); R. Sonnenfeld and P. K. Hansma, Science 232, 211 (1986).
18. S.-I. Park and C. F. Quate, Appl. Phys. Lett. 48, 112 (1986).
19. E. C. Teague, "Room Temperature Gold-Vacuum-Gold Tunneling Experiments," University Microfilms International, Ann Arbor, Michigan (1978).
20. J. M. Soler, A. M. Baro, N. Garcia, and H. Rohrer, Phys. Rev. Lett. 57, 444 (1986); R. J. Wilson and S. Chiang, to be published.